Chapter 12

Rethinking homo economicus
ISBN: 978-9915-704-23-4
DOI: 10.62486/978-9915-704-23-4.Ch12
Pages: 155-166

Drought Forecasting Using Feed Forward Multi-Layer Perceptron (MLP) Neural Networks

Pronóstico de sequías mediante redes neuronales de perceptrón multicapa (MLP) de avance

Ali Ssubhi Alhumaima[1], Raed H. C. Alfilh[2], Hussein Alkattan[3,4], Mostafa Abotaleb[5], Klodian Dhoska[6]

[1]Electronic and Computer Center, University of Diyala. Baqubah MJJ2+R9G, Iraq.

[2]Refrigeration & Air-Conditioning Technical Engineering Department, College of Technical Engineering, The Islamic University. Najaf, Iraq.

[3]Department of System Programming, South Ural State University. Chelyabinsk, Russia.

[4]Directorate of Environment in Najaf, Ministry of Environment. Najaf, Iraq.

[5]Engineering School of Digital Technologies, Yugra State University. Khanty-Mansiysk, 628012, Russia.

[6]Department of Mechanics, Polytechnic University of Tirana. Tirana, Albania.

ABSTRACT

For the past decades, drought has affected the natural environment of large areas of the Euphrates and Tigris Rivers Basin (ETRB), therefore drought monitoring and identification plays an important role in the planning and management of natural resources and water resource systems in the region. Standardized precipitation index (SPI) has been used as a standard tool to identify and monitor drought occurrences. However, to reduce and mitigate the adverse effects of drought impacts, effective forecasting of future droughts is necessary. In this paper, average long-term monthly rainfall data for five stations covering both the dry and wet seasons from the Eastern part of the ETRB have been used to derive the SPI values for durations of 3, 6, 9 and 12 months. These drought indicators were used as time series for drought forecasting for the basin using the multi-layer artificial neural networks model. The results show that more accurate predictions are achieved using SPI for longer durations, i.e. 12 months.

Keywords: Drought Monitoring; Euphrates-Tigris River Basin (ETRB); Standardized Precipitation Index (SPI); Drought Forecasting; Artificial Neural Networks (ANN); Rainfall Data; Time Series Analysis.

RESUMEN

Durante las últimas décadas, la sequía ha afectado el entorno natural de extensas zonas de la Cuenca de los Ríos Éufrates y Tigris (ETRB). Por lo tanto, el monitoreo e identificación de sequías desempeña un papel importante en la planificación y gestión de los recursos naturales y los sistemas hídricos de la región. El índice de precipitación estandarizado (IPE) se ha utilizado como herramienta estándar para identificar y monitorear la ocurrencia de sequías. Sin embargo, para reducir y mitigar los efectos adversos de la sequía, es necesario un pronóstico efectivo de futuras sequías. En este trabajo, se utilizaron datos promedio de precipitación mensual a largo plazo de cinco estaciones que abarcan tanto la estación seca como la húmeda de la parte oriental de la ETRB para obtener los valores del IPE para periodos de 3, 6, 9 y 12 meses. Estos indicadores de sequía se utilizaron como series temporales para el pronóstico de sequías en la cuenca mediante el modelo de redes neuronales artificiales multicapa. Los resultados muestran que se obtienen predicciones más precisas utilizando el IPE para periodos más largos, es decir, 12 meses.

Palabras clave: Monitoreo de Sequías; Cuenca de los Ríos Éufrates-Tigris (ETRB); Índice de Precipitación Estandarizado (SPI); Pronóstico de Sequía; Redes Neuronales Artificiales (ANN); Datos de Lluvia; Análisis de Series de Tiempo.

INTRODUCTION

Drought occurrence is a normal climate feature and drought is a gradual phenomenon.(1) For severe cases, drought can last for many years, which can have devastating effects on agriculture and water supply.(2) However, it is difficult to determine the onset and end of a drought. A drought can be short, lasting only a few months, or it can be persistent for years before the climatic conditions return to normal.(3) An effective monitoring system helps to mitigate the impact of droughts.(4) Timely monitoring of droughts can help to establish an early warning system.(5) Evaluation of current drought condition and forecasting of future drought occurrence in an area is important in mitigating the impacts of droughts.(6)

Drought indices are normally used to evaluate and forecast drought occurrence.(7) Commonly used drought indices are the standardized precipitation index (SPI), the Palmer index and the crop moisture index.(8) For this study, the SPI method has been used to derive drought index as this method is standardized and ensures independence from geographical position as the index in question is calculated with respect to the average precipitation in the same place.(9) This characteristic makes the SPI useful as a primary drought index because it is simple, spatially invariant in its interpretation and probabilistic nature allow it to be used in risk and decision making analysis.(10)

SPI prediction is a critical issue that has attracted much attention in recent decades all over the world in order to carry out hydrological modelling in arid and semi-arid regions.(11) Today, more non-linear models are applied to prediction. In previous studies, Dahamsheh et al.(12), Azadi et al.(13), and Rezaeian-Zadeh et al.(11) used artificial neural networks (ANNs), and El-Shafie et al.(14), Sanikhani et al.(15), Valizadeh et al.(16), and Choubin et al.(17) successfully applied the adaptive neuro-fuzzy inference system (ANFIS) to predict precipitation. In eastern Australia, Deo et al.(18) investigated the application of the ANN model for the prediction of monthly SPIs using hydro meteorological parameters and climate indices. The results showed that the ANN model is a useful data-driven tool for forecasting monthly SPIs. In the Awash River Basin (Ethiopia), Belayneh et al.(19) forecasted the long-term SPI drought using wavelet neural networks. The forecasted results indicated that the coupled wavelet neural network (WA-ANN) models were better than all the other models in this study for forecasting SPI 12 and SPI 24 values. Ruigar et al.(20) predicted the precipitation in the Golestan dam watershed using climate indices: their results indicated that the MLP model is capable of accurately predicting monthly maximum precipitation.

In the present study, the utility of ANN approach for medium and long term forecasting of both the likelihood of drought events and their severity was examined In the ETRB. Neural network models were developed using the multilayer perceptron neural network approach (MLPNN) with SPI as the drought indicator. Different combinations of past rainfall, temperature and evapotranspiration values were used for forecasting drought at different lead times.

Study Area

The study area which includes part of the Euphrates Tigris Rivers Basin (ETRB), is a trans boundary area distributed mainly between Iraq, Turkey, and the Islamic Republic of Iran (figure 1), located approximately between 41°05′-48°07′E and 38°38′-48°07′N, with a total area of 251,368 km2.[21] The study area contains the basins of five tributaries of the Tigris River within the Iraqi territory which feed the river. Taken in a sequence they are: Khabour tributary at the entry point of the Tigris River at Fesh-Khabor, Greater Zab, Lesser Zab, Al-Adhaim, and finally Diyala tributary which ends in the Tigris only 30 kilometres south of Baghdad city.[21] The terrain is mountainous in the northeast and becomes flat gradually as moving to the southwest with elevation ranging from -148 m to 4064 m as can be seen from the results of the Advanced Spaceborne Thermal Emission and Reflection Radiometer (ASTER) Global Digital Elevation Model (DEM).

The climate varies significantly along the study area, but is generally characterized as wet during the winter and spring (October to May), with mean annual precipitation and temperature ranging between 570 mm and 14,3 °C respectively in the highlands of the Greater Zab river basin in the north and between 420 mm and 36°C respectively in the lowlands of Diyala river basin in the south.[22]

This area was chosen mainly because of its location in transitional climatic zones, from arid and semi-arid to humid environments, and because of its vegetation diversity and the large spread of the rain-fed lands,[23] all these factors making it highly responsive to variations in the precipitation and temperature levels[24] and therefore it is ideal to study the relationship between climate variables and SPI.

METHOD

Precipitation, Temperature and Evapotranspiration Dataset

The climate datasets used in this paper which are the observations of monthly total precipitation, monthly mean surface air temperatures (at 2 m above surface), and monthly mean evapotranspiration are obtained from the University of East Anglia (UEA)/ Climatic Research Unit (CRU) (Version 4,01), which provides monthly global gridded high spatial resolution (0,5 Degree) land dataset for the period 1901-2016.

Digital Elevation Maps

The digital elevation model (DEM) that used in this paper was extracted from the Advanced Spaceborne Thermal Emission and Reflection Radiometer (ASTER) Global Digital Elevation Model (DEM) with a 30 meter grid spatial resolution and 1×1 degree tiles (https://asterweb.jpl.nasa.gov/gdem.asp) (METI/NASA). The ASTER GDEM is distributed as Geo-referenced Tagged Image File Format (GeoTIFF) files, and in geographic coordinates (latitude, longitude).

Multi-layer Perceptron Artificial Neural Networks

Studying artificial neural network was inspired mainly from the biological learning system, the biological model is composed of complex layers of interconnected neurons. In effect, the human brain is composed of approximately 1011 neurons, each one has an average of 103 connections. It is believed that the considerable calculation power of the brain is a result of the parallel and distributed processing performed by these neurons.

The artificial neuron has generally multiple inputs and a single output. Actions of excitatory synapses are illustrated by the coefficients called synaptic weights; these weights are coupled with all inputs. The numerical values of these coefficients are adjusted in the learning phase (figure 2).

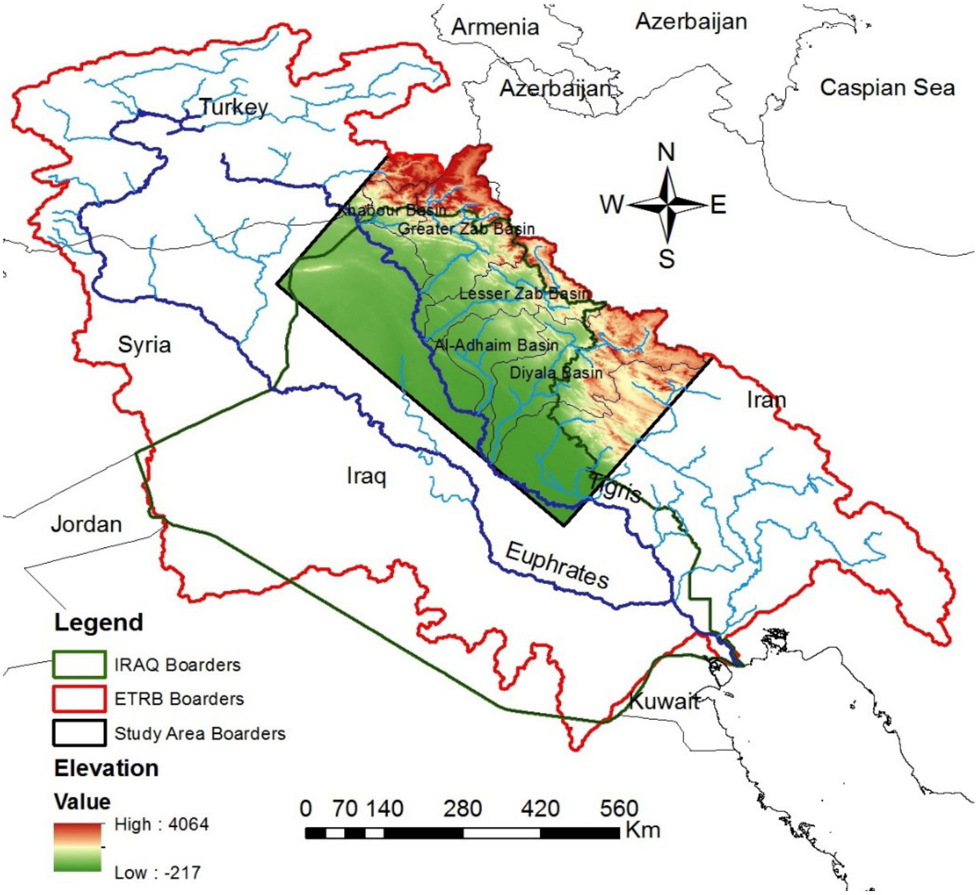

Figure 1. Study area with elevation level according to the ASTER global DEM

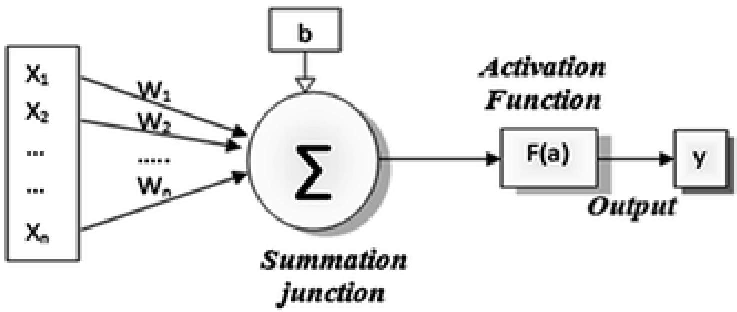

Figure 2. Mathematical model of the formal neuron

The formal neuron that is given in the figure above has n inputs denoted as {X1, X2…Xn}. Each line that connects these inputs to the summation junction is assigned a weight, denoted as {W1, W2…Wn}. The output y of the neuron is given by the formula:

$$f=\sum_{i=1}^{n} x_i \cdot w_i + b \qquad (1)$$

One of the most important parts of a neuron is its activation function F(a). In this work, a sigmoid function has been used, because of it's nonlinearity of making it possible to approximate any function.

A Multi-Layer Perceptron (MLP) consists of a number of artificial neurons interconnected, this network is organized in the form of layers. The first and last layers are called, respectively, the input and output layers. Layers that are neither input nor output are known as hidden layers. MLP are especially trained using the back-propagation algorithm, which aims at minimizing the global error measured at the output layer, by the relation below:

$$e(t) = y_d(t) - y_m(t) \quad (2)$$

Where yd(t) denotes the desired output, and ym(t) the measured output of the neuron.

The BP algorithm uses an iterative supervised learning procedure, where the MLP is trained with a set of predefined inputs and outputs. And, the global error Eg(t) is calculated by equation (3), this error can be minimized by the gradient descent technique.

$$E_g(t) = \frac{1}{2}\sum_{i=1}^{n}(y_{d,i}(t) - y_{m,i}(t))^2 \quad (3)$$

The most efficient algorithm to optimize the global error Eg(t) is that of gradient descent.

Standardized Precipitation Index (SPI)

More complex calculations were needed in the calculation of Standardized Precipitation Index (SPI). The computation of the SPI drought index for any location is based on the long-term precipitation record (at least 30 years) cumulated over a selected time scale. This long-term precipitation time series is then fitted to a gamma distribution, which is then transformed through an equal probability transformation into a normal distribution. Positive SPI values indicate wet conditions with greater than median precipitation, and negative SPI values indicate dry conditions with lower than median precipitation.

In most cases, the probability distribution that best models observational precipitation data is the Gamma distribution. The gamma distribution is defined by its frequency or probability density function:

$$g(x) = \frac{1}{\beta^{\alpha}\,\Gamma(\alpha)} x^{\alpha-1} e^{-x/\beta}, \text{for x} > 0 \quad (4)$$

Where α > 0 is the shape parameter, β > 0 is the scale parameter, and x > 0 is the amount of precipitation. Γ(α) is the Gamma function, which is defined by the integral:

$$\Gamma(\alpha) = \int_0^{\alpha} \gamma^{\alpha-1} e^{-\gamma} d\gamma. \quad (5)$$

Computation of the SPI involves fitting a gamma probability density function to a given frequency distribution of precipitation total for a station. The maximum likelihood solutions are used to optimally estimate α and β for n precipitation observations:

$$\alpha = \frac{1}{4A}\left(1+\sqrt{1+\frac{4A}{3}}\right); \quad \text{where } A = ln(\bar{x}) - \frac{\sum ln(x)}{n} \text{ and } \beta = \frac{\bar{x}}{\alpha} \qquad (6)$$

The cumulative probability G(x) is given by:

$$G(x) = \int_0^x g(x)\,dx = \frac{1}{\beta\Gamma(\alpha)} = \int_0^x x^{\alpha-1} e^{-x/\beta} dx \qquad (7)$$

The Gamma function is not defined by x = 0, and since there may be no precipitation, the cumulative probability becomes:

$$H(x) = q + (1-q)\,G(x) \qquad (8)$$

Where q is the probability of no precipitation. H(x) is the cumulative probability of precipitation observed. The cumulative probability is then transformed to the standard normal random variable Z with mean zero and variance of one, which is the value of the SPI. SPI is categorized based on their range values is shown in table 1.

Table 1. Drought classification based on SPI

SPI values	Class	SPI values	Class
2,00 and more	Extremely wet	-2,00 and less	Extremely dry
1,50 to 1,99	Very wet	-1,50 to -1,99	Very dry
1,00 to 1,49	Moderately wet	-1,00 to -1,49	Moderately dry
0,99 to 0,00	Normal	0,00 to -0,99	Near normal

Evaluation of the performance of the models

The coefficient of correlation (R2), root mean square error (RMSE) and mean absolute error (MAE) for each combination of input and hidden neurons was calculated. The combination having a maximum coefficient of correlation and minimum root mean square error was chosen as an optimal network.

Software

All the results presented in this paper have been calculated using MATLAB programming language version 8.5.0.197613 (R2023a), whereas the ArcGIS version 10.8.2 has been used to simulate the results as geographical maps. The Euphrates-Tigris river basin shapefiles used within the ArcGIS has been projected using the maps presented in the inventory of shared water resources in western Asia by the United Nations Economic and Social Commission for Western Asia.

RESULTS AND DISCUSSION

In the present study, the neural network models were developed to forecast drought using the feed forward training with standard back propagation algorithm.(25,26,27) The available data were split into two parts, the data set from 1965 to 1999 was used to estimate the model parameters and the data from 2000 to 2010 was used to check the forecast accuracy.[28,29,30] The forecast lead times varied from 1 to 12 months. Because it is the medium-range and the long-range forecasts that are critical for drought preparedness, we further discuss only the results of forecasting with a lead time of 3 months and longer.[31,32,33] It is also virtually impossible to illustrate all results for all stations. We therefore primarily use the results from the worst drought affected station (Lesser Zab) as per the SPI analysis results to illustrate the main points.[34,35,36] The statistics presented in table 2 indicate that for a lead time of 3 months, models 1, 2, 5 and 6 have performed better than 3 and 4.

Table 2. Results of SPI forecasting (three months lead time) at Lesser Zab station

Model	Architecture	Training				Validation			
		R	R^2	MAE	RMSE	R	R^2	MAE	RMSE
1	(P) 1-15-1	0,97	0,91	0,19	0,24	0,93	0,81	0,17	0,65
2	(P+E) 2-15-1	0,97	0,91	0,18	0,23	0,97	0,94	0,15	0,17
3	(T) 2-13-1	0,89	0,71	0,32	0,40	073	0,22	0,34	0,50
4	(T+E) 2-10-1	0,82	0,38	0,41	0,52	0,87	0,21	0,33	0,42
5	(P+T) 2-13-1	0,95	0,87	0,22	0,28	0,87	0,68	0,22	0,32
6	(P+T+E) 3-11-1	0,98	0,94	0,15	0,20	0,99	0,96	0,11	0,13

It was also observed that the model 2 (Rainfall and potential evapotranspiration) performed better than model 1 with only rainfall as input.

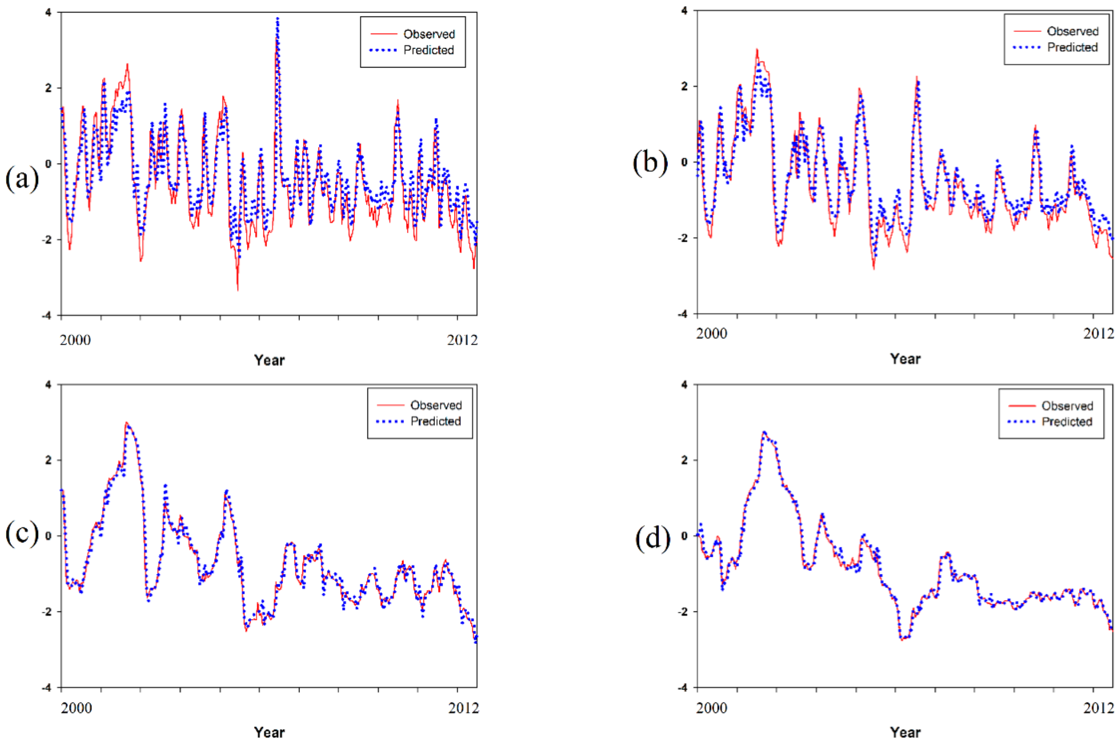

Figure 3. Comparison of observed and forecasted SPI at the Lesser Zab station with lead times of 3 months (a), 6 months (b), 9 months (c) and 12 months (d) from 2000-2012

Similarly, the model 6 (Rainfall, Temperature and potential evapotranspiration) performed better than model5 (Rainfall and Temperature). This emphasized the importance of potential evapotranspiration in drought forecasting. The forecasts significantly improved with model 6, where the R2 values for training and validation periods were 0,94 and 0,96 respectively. Models 3 and 4 with Temperature as a single input and different combinations of other inputs had not resulted in accurate forecasts. In case of drought forecasting with 6 months and 9 months lead times, model 4 and model 5 didn't work well at all like the other models. The R2 values were low and the RMSE and MAE values were high in both the cases as compared to the 3 month and 12 month lead times. The forecast with 12 month lead time indicated that all the six models worked and the best model the architecture was 7-7-1 with RMSE and MAE of 0,1, 0,07 in training and 0,12, 0,1 in validation respectively.(37,38)

Figure 3 displays the observed time series of the SPI values against the forecasted ones with the lead times of 3, 6, 9 and 12 months. In all cases, the significance level of R2 is 1 %. The results effectively illustrated the high accuracy of medium and long range forecasts of SPI at Lesser Zab station. The results at other stations were broadly similar. From the above maps, it was observed that SPI forecasts for 9 and 12 months were better than that for 3 and 6 months.

CONCLUSIONS

The paper described the procedure for SPI drought forecasting using the ANN and its application in the ETRB. Different combinations of the past precipitation, temperature and potential evapotranspiration were used as predictors. 20 different models were tested for each drought index at five rainfall stations in this region with lead times of 3 to 12 months. The SPI with 9 months and 12 months lead times forecasted better than other lead times at all rainfall stations. The best models had R^2 values of 0,93-0,99 for a lead time of 3 months. The models including potential evapotranspiration as an input performed better than the models considering rainfall and temperature alone. The structure of the model inputs (previous precipitation, temperature and potential evapotranspiration) does not vary with the lead time, which makes the models convenient for operational purposes like management of water resources.

BIBLIOGRAPHIC REFERENCES

1. Wang Z, Chang J, Wang Y, Yang Y, Guo Y, Yang G, et al. Temporal and spatial propagation characteristics of meteorological drought to hydrological drought and influencing factors. Atmos Res. 2024;299:107212. https://doi.org/10.1016/j.atmosres.2023.107212

2. Savari M, Eskandari Damaneh H, Eskandari Damaneh H. Managing the effects of drought through the use of risk reduction strategy in the agricultural sector of Iran. Clim Risk Manag. 2024;45:100619. https://doi.org/10.1016/j.crm.2024.100619

3. Wilhite DA, Sivakumar MVK, Pulwarty R. Managing drought risk in a changing climate: The role of national drought policy. Weather Clim Extrem. 2014;3:4-13. https://doi.org/10.1016/j.wace.2014.01.002

4. Abotaleb M, Makarovskikh T, Ali Subhi A, Alkattan H, Adebayo AO. Forecasting and modeling on average rainwater and vapor pressure in Chelyabinsk Russia using deep learning models. IET Conf Proc. 2023;2022:362-7. https://doi.org/10.1049/icp.2023.0582

5. Vicente-Serrano SM, et al. A near real-time drought monitoring system for Spain using automatic weather station network. Atmos Res. 2022;271:106095. https://doi.org/10.1016/j.atmosres.2022.106095

6. Nandgude N, Singh TP, Nandgude S, Tiwari M. Drought Prediction: A Comprehensive Review of Different Drought Prediction Models and Adopted Technologies. Sustainability. 2023;15:11684. https://doi.org/10.3390/su151511684

7. Ahmadi M, Etedali HR, Kaviani A, Tavakoli A. Evaluation of meteorological drought indices using remote sensing. J Atmos Sol-Terr Phys. 2024;265:106387. https://doi.org/10.1016/j.jastp.2024.106387

8. Asadi Zarch MA, Sivakumar B, Sharma A. Droughts in a warming climate: A global assessment of Standardized precipitation index (SPI) and Reconnaissance drought index (RDI). J Hydrol. 2015;526:183-95. https://doi.org/10.1016/j.jhydrol.2014.09.071

9. Vazini Ahghar E, Shah-Hosseini R, Nazari B, Dodangeh P, Mousavi SM. Assessment of Drought in Agricultural Areas by Combining Meteorological and Remote Sensing Data. In: IECG 2022. Basel: MDPI; 2023. p. 28.

10. Hong D, Hong KA. Drought Forecasting Using MLP Neural Networks. In: 2015 8th International Conference on u- and e-Service, Science and Technology (UNESST). IEEE; 2015. p. 62-5.

11. Rezaeian-Zadeh M, Tabari H, Abghari H. Prediction of monthly discharge volume by different artificial neural network algorithms in semi-arid regions. Arab J Geosci. 2013;6:2529-37. https://doi.org/10.1007/s12517-011-0517-y

12. Dahamsheh A, Aksoy H. Artificial neural network models for forecasting intermittent monthly precipitation in arid regions. Meteorol Appl. 2009;16:325-37. https://doi.org/10.1002/met.127

13. Azadi S, Sepaskhah AR. Annual precipitation forecast for west, southwest, and south provinces of Iran using artificial neural networks. Theor Appl Climatol. 2012;109:175-89. https://doi.org/10.1007/s00704-011-0575-9

14. El-Shafie A, Jaafer O, Seyed A. Adaptive neuro-fuzzy inference system based model for rainfall forecasting in Klang River, Malaysia. Int J Phys Sci. 2011;6:2875-88.

15. Sanikhani H, Kisi O. River Flow Estimation and Forecasting by Using Two Different Adaptive Neuro-Fuzzy Approaches. Water Resour Manag. 2012;26:1715-29. https://doi.org/10.1007/s11269-012-9982-7

16. Valizadeh N, El-Shafie A. Forecasting the Level of Reservoirs Using Multiple Input Fuzzification in ANFIS. Water Resour Manag. 2013;27:3319-31. https://doi.org/10.1007/s11269-013-0349-5

17. Choubin B, Khalighi-Sigaroodi S, Malekian A, Kişi Ö. Multiple linear regression, multi-layer perceptron network and adaptive neuro-fuzzy inference system for forecasting precipitation based on large-scale climate signals. Hydrol Sci J. 2016;61:1001-9. https://doi.org/10.1080/02626667.2014.966721

18. Deo RC, Şahin M. Application of the Artificial Neural Network model for prediction of monthly Standardized Precipitation and Evapotranspiration Index using hydrometeorological

parameters and climate indices in eastern Australia. Atmos Res. 2015;161-162:65-81. https://doi.org/10.1016/j.atmosres.2015.03.018

19. Belayneh A, Adamowski J, Khalil B. Short-term SPI drought forecasting in the Awash River Basin in Ethiopia using wavelet transforms and machine learning methods. Sustain Water Resour Manag. 2016;2(1):87-101. https://doi.org/10.1007/s40899-015-0040-5

20. Ruigar H, Golian S. Prediction of precipitation in Golestan dam watershed using climate signals. Theor Appl Climatol. 2016;123:671-82. https://doi.org/10.1007/s00704-015-1377-2

21. Alhumaima AS, Abdullaev SM. Forecasting Lower Tigris Basin Landscapes' Vegetation Response to Regional and Global Climate Variability. In: Advances in Science, Technology and Innovation. 2023. p. 39-42.

22. Alhumaima AS, Abdullaev SM. The sensitivity of vegetation in the lower Tigris basin landscapes to regional and global climate variability. Sci Rev Eng Environ Stud. 2021;30:159-70. https://doi.org/10.22630/PNIKS.2021.30.1.14

23. Alhumaima AS, Abdullaev SM. Tigris Basin Landscapes: Sensitivity of Vegetation Index NDVI to Climate Variability Derived from Observational and Reanalysis Data. Earth Interact. 2020;24:1-18. https://doi.org/10.1175/EI-D-20-0002.1

24. Alqahtani F, et al. A hybrid deep learning model for rainfall in the wetlands of southern Iraq. Model Earth Syst Environ. 2023;9:4295-312. https://doi.org/10.1007/s40808-023-01754-x

25. Harris I, Jones PD, Osborn TJ, Lister DH. Updated high-resolution grids of monthly climatic observations. Int J Climatol. 2014;34:623-42. https://doi.org/10.1002/joc.3711

26. Montesinos López OA, Montesinos López A, Crossa J. Fundamentals of Artificial Neural Networks and Deep Learning. In: Multivariate Statistical Machine Learning Methods for Genomic Prediction. Springer International Publishing; 2022. p. 379-425.

27. Rosenblatt F. The perceptron: A probabilistic model for information storage and organization in the brain. Psychol Rev. 1958;65:386-408. https://doi.org/10.1037/h0042519

28. Hornik K, Stinchcombe M, White H. Multilayer feedforward networks are universal approximators. Neural Netw. 1989;2:359-66. https://doi.org/10.1016/0893-6080(89)90020-8

29. Alkattan H, Abdullaev SME, El-Kenawy EM. The "Climate in Weathers" approach to processing of meteorological series in Mesopotamia: Assessment of climate similarity and climate change using data mining. J Intell Syst Internet Things. 2023;10(1):48-65. https://doi.org/10.54216/JISIoT.100104

30. Mckee TB, Doesken NJ, Kleist J. The relationship of drought frequency and duration to time scales. In: Proceedings of the 8th Conference on Applied Climatology. Anaheim (CA): American Meteorological Society; 1993 Jan 17-22. p. 179-84.

31. Zuo D-D, Hou W, Zhang Q, Yan P-C. Sensitivity analysis of standardized precipitation index to climate state selection in China. Adv Clim Change Res. 2022;13:42-50. https://doi.org/10.1016/j.accre.2021.11.004

32. Belayneh A, Adamowski J. Standard Precipitation Index Drought Forecasting Using Neural Networks, Wavelet Neural Networks, and Support Vector Regression. Appl Comput Intell Soft Comput. 2012;2012:1-13. https://doi.org/10.1155/2012/794061

33. Pazhanivelan S, Geethalakshmi V, Samykannu V, Kumaraperumal R, Kancheti M, Kaliaperumal R, et al. Evaluation of SPI and Rainfall Departure Based on Multi-Satellite Precipitation Products for Meteorological Drought Monitoring in Tamil Nadu. Water. 2023;15:1435. https://doi.org/10.3390/w15071435

34. Pieper P, Düsterhus A, Baehr J. A universal Standardized Precipitation Index candidate distribution function for observations and simulations. Hydrol Earth Syst Sci. 2020;24:4541-65. https://doi.org/10.5194/hess-24-4541-2020

35. Di Nunno F, de Marinis G, Granata F. Analysis of SPI index trend variations in the United Kingdom - A cluster-based and bayesian ensemble algorithms approach. J Hydrol Reg Stud. 2024;52:101717. https://doi.org/10.1016/j.ejrh.2024.101717

36. Sharma J, Sonia K, Kumar K, Jain P, Alfilh RHC, Alkattan H. Enhancing intrusion detection systems with adaptive neuro-fuzzy inference systems. Mesopotamian J Cybersecurity. 2025;5(1):1-10. https://doi.org/10.58496/MJCS/2025/001:contentReference[oaicite:0]{index=0}

37. Khodadadi E, Towfek SK, Alkattan H. Brain tumor classification using convolutional neural network and feature extraction. Fusion Pract Appl. 2023;13(2):34-41. https://doi.org/10.54216/FPA.130203:contentReference[oaicite:1]{index=1}

38. METI/NASA. ASTER Global Digital Elevation Model, version 2. NASA EOSDIS Land Processes DAAC; 2011. https://asterweb.jpl.nasa.gov/gdem.asp.